Nuclear Instruments and Methods in Physics Research A 616 (2010) 188–192

Contents lists available at ScienceDirect

Nuclear Instruments and Methods in Physics Research A

journal homepage: www.elsevier.com/locate/nima

Evolution of surface roughness in silicon X-ray mirrors exposed to a low-energy ion beam

E. Ziegler [a,*], L. Peverini [a], N. Vaxelaire [a], A. Cordon-Rodriguez [a], A. Rommeveaux [a], I.V. Kozhevnikov [b], J. Susini [a]

[a] European Synchrotron Radiation Facility, 38043 Grenoble cedex, France
[b] Institute of Crystallography, Moscow 119333, Russian Federation

ARTICLE INFO

Available online 6 January 2010

Keywords:
X-ray
Mirror
Surface roughness
Nanofocusing
Ion beam
Polishing

ABSTRACT

The possibility of smoothening aspherical X-ray mirrors by irradiation of the surface with a low-energy ion beam is investigated. Nanofocusing being the primary application of these mirrors the ion beam conditions must be optimized to achieve a surface roughness of the order of 0.1–0.2 nm. To address this issue a first study was performed on silicon flat substrates etched using ion energies ranging from 400 to 1200 eV. A second study consisted of eroding the silicon surface while varying the ion grazing incidence angle between 10° and 90° for a fixed value of the ion energy. The surface topography of the samples was characterized at various scales using atomic force microscopy (probed area: $1-10\,\mu m^2$), interferential optical microscopy (probed area: $1\,mm^2$) and X-ray scattering (probed area: $100\,mm^2$). Finally, a study by AFM of the evolution of the surface finish level of a silicon mirror after ion erosion at various depth values up to 10 μm allowed a trade off to be found between total etch time and the finish quality level in view of profiling a highly aspherically shaped mirror starting from a flat surface.

1. Introduction

By generating X-ray nanofocused beams with high photon density, synchrotron and free-electron laser facilities are expecting a substantial improvement in the performance of the X-ray based analysis tools. For instance, a spatial resolution of a few tens of nanometers will be routinely available in X-ray imaging. In fluorescence nanoscopy both a lower detection limit and a higher spatial resolution are foreseen [1]. Such a goal implies that mirrors with strong curvature ($R \leq 10\,m$) and asphericity (eccentricity close to unity) and with figure errors of the order of a nanometer can be manufactured [2]. In addition the mirror surface roughness must remain as low as possible (0.1–0.2 nm) to minimize the amount of X-ray light scattered around the focal spot. Low roughness at high-spatial frequency is also essential to preserve the specular reflectance of the multilayer coating [3] eventually deposited on the mirror surface to increase the numerical aperture through a higher incidence angle, thus lowering the diffraction limit threshold. Alternatively, for X-ray experiments that need to vary the photon energy over a large range, the mirror is coated with a single (metal) film of high density, for which the replication process of the topography of the substrate underneath and of the film surface need to be assessed [4]. Due to its thermal properties, long term stability and overall cost-performance, single crystal silicon was selected as X-ray mirror substrate [5]. Nowadays there is a growing interest for the use of ion beams for smoothening mirror surfaces [6]. However, depending on the ion beam operation conditions and on the composition and topography of the initial sample, ion irradiation may result in very different topographies including rough, smooth and patterned (ripples, nanodots, etc.) surfaces [7]. This paper investigates irradiation parameters, such as ion incidence angle, energy, erosion time and substrate material and geometry, to eventually focus on the conditions corresponding to surface smoothing. For this occasion an experimental station initially used to perform real time X-ray reflectometry experiments during growth and erosion [8] and the tools used to investigate the surface topography will be described. This work is part of a global project aimed at optimizing both mirror figure and surface finish, an old challenge that is nowadays extended to X-ray mirror optics. A companion paper addressing the issue of ion beam figuring of strongly curved surfaces can be found in the same proceedings [9].

2. Experimental setup

2.1. Ion beam irradiation

The experiments were performed at an experimental facility developed and installed at the ESRF bending-magnet beamline

* Corresponding author. Tel.: +33 4 7688 2170; fax: +33 4 7688 2957.
E-mail address: ziegler@esrf.fr (E. Ziegler).

0168-9002/$ - see front matter © 2010 Elsevier B.V. All rights reserved.
doi:10.1016/j.nima.2009.12.062

BM5. The setup consists of a vacuum chamber with a base pressure of 3.6×10^{-7} h Pa equipped with a magnetron sputter source for film deposition and a broad ion beam source for etching. In the latter case, plasma is generated by electron cyclotron resonance (ECR). Microwave pulses with a frequency of 2.45 GHz are introduced in a cavity and the plasma is maintained by the field of a quadrupole located around it. The extraction of the ions from the cavity and their introduction in the process chamber are achieved by applying a voltage to a set of grids. The ion energy, defined by the anode voltage, can be varied between 0 and 1600 V, while an extractor grid, typically set to a voltage of −200 V, monitors the extraction. The ECR ion source has the advantage of producing ions of low energy. The ion beam has a Gaussian profile with a 15° divergence so that the beam size at the exit aperture has a 25 mm diameter. Most experiments described below used Argon gas to produce the ion plasma. Further etching experiments were combined with mirror figuring that required an operation over several hours. They required a gas mixture composed of 90% Ar and 10% air, the latter avoiding the metallization of the ceramic spacer that insulates the grids. The proportion between gases was maintained constant using two mass flow meters set in a master–slave mode while a valve regulating the conductance between the chamber and the exhaust pumping system maintained the total pressure to a value of 1×10^{-3} h Pa. The sample (dimension 25×50 mm^2, 7 mm thick) was mounted onto a holder integral to a rotating vacuum feedthrough so that the angle of incidence of the ion beam with respect to the sample surface could be varied from grazing to normal incidence. For the surface smoothening study as a function of the ion grazing angle (10–90°) and energy (400–1200 eV) presented in Section 3, the erosion rates ranged from 11 to 44 pm/s. For surface figuring experiments [9] the ion beam setup was set to increase the erosion rate at 600 eV ion energy and 70° incidence angle. In this case, at a distance of 100 mm between the source and the Si sample, an ion current of 1 mA/cm^2 was generated, resulting in an erosion rate of the order 1 nm/s.

2.2. Surface topography characterization

The topography of a surface is fully characterized by the power spectral density (PSD) [10]. The PSDs of the various treated surfaces were obtained either with a local probe such as an atomic force microscope (AFM) looking at an area of 1–10 μm^2 or an interferential microscope Promap 512 (Micromap) probing an area in the order of 1 mm^2 or, to get a much greater statistics, with X-ray diffuse scattering (XRS) probing an area in the order of 100 mm^2. The interference microscope covers the mid-spatial frequencies $[10^{-3}, 2]\,\mu m^{-1}$ while AFM and XRS methods give access to a higher spatial frequency range ($[1,100]\,\mu m^{-1}$) corresponding to the mirror surface finish [11]. Most characterizations presented here were performed ex-situ at the ESRF Surface Science Laboratory using an AFM (Nanoscope III, Veeco). The substrates used in our experiments consist of superpolished silicon substrates of flatness better than $\lambda/15$ (λ=633 nm) and with an initial surface root-mean-square (rms) roughness of 0.15 nm in the above-mentioned spatial frequency range. For such smooth surfaces AFM measurements are difficult to perform and the contact mode was preferred owing to a lower noise. The raw images were treated using the WSxM software program [12] that allowed us to derive the PSD and the correlation functions. The rms roughness over a given spatial frequency range $[p_{min}, p_{max}]$ can be calculated from the 2-dimensional PSD function according to the following expression:

$$\sigma^2 = 2\pi\int_{p_{min}}^{p_{max}} PSD_{2D}(p)pdp$$

Some samples were also characterized by X-ray reflectometry to quantitatively evaluate the presence of an adhesion layer and the depth density profile near the sample surface as a function of the etched depths. The X-ray signal at a 12 keV energy was recorded using a $LaCl_3$ scintillator detector.

3. Results and discussion

A series of parameters of the ion beam irradiation expected to affect the mirror surface were investigated: ion incidence angle, ion energy, erosion time, and substrate material and geometry. The samples were etched to a depth varying from 20 to 80 nm, a range of depth values relevant for mirror surface figure corrections. At low grazing incidence (10°) with respect to the sample surface the AFM images showed the presence of ripples irrespective of the ion energy (see Fig. 1). When varying the energy from 600 to 1200 eV and with a same erosion time of 30 min the distance of correlation was shown to increase from 36 nm at 600 eV to 54 nm at 1200 eV, in agreement with other authors' findings. Differences were observed after irradiation between the surface morphology of a wafer substrate and of a superpolished sample, as illustrated in Fig. 2 for an irradiation of 30 min at an energy of 800 eV and an angle of 10°. Possible causes include a higher temperature for the thinner (0.65 mm) wafer as compared to the 7 mm thick polished substrate and the use of different chemical-mechanical polishing processes during

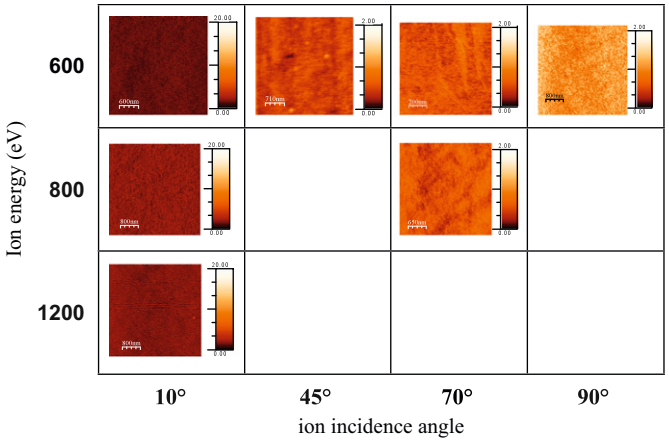

Fig. 1. AFM images recorded at the center of the irradiated zone for a series of superpolished silicon substrates irradiated at various grazing angles (10°, 45°, 70°, 90°) and ion energy (600, 800, 1200 eV).

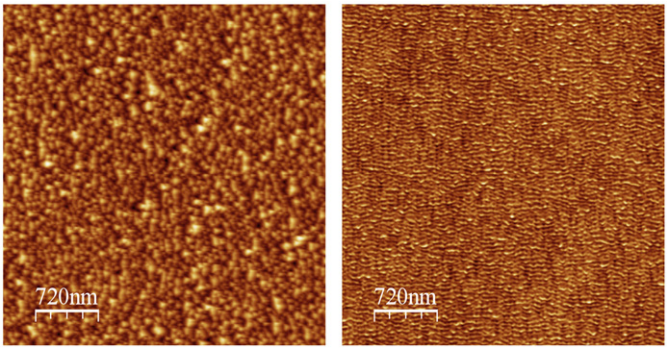

Fig. 2. Comparison of two AFM images recorded on a Si wafer (left) and on a thick polished Si substrate (right) after irradiation during 30 mn at a grazing angle of 10° with an ion energy of 800 eV.

substrate manufacturing, leading to different amorphization depth and oxidation of the silicon close to the surface. A further study was performed at higher incidence angles between 45° and 90° (normal incidence). The surfaces were investigated by AFM. All images were taken in the center of the irradiated zones. At 600 eV smooth images were obtained for incidence angles between 45° and 70° (σ_{rms}=0.15 nm at 45°). Fig. 3 compares the PSD derived from the AFM images obtained at 10°, 45° and 90°. In contrast to the cases at 10° and 90°, the PSD at 45° does not exhibit any preferential frequency. The peak observed at 10° is less pronounced than at 90°. Notice that the PSDs should only be compared in the common spatial frequency part $[1\times10^{-3},3.69\times10^{-2}]\,nm^{-1}$. Fig. 1 presents a summary of the various AFM data obtained with the superpolished substrates used for mirror fabrication, while Fig. 4 shows a similar study on Si wafers. In both cases the lowest roughness among our limited number of angle–energy conditions performed was found at 600 eV for an angle of 70°.

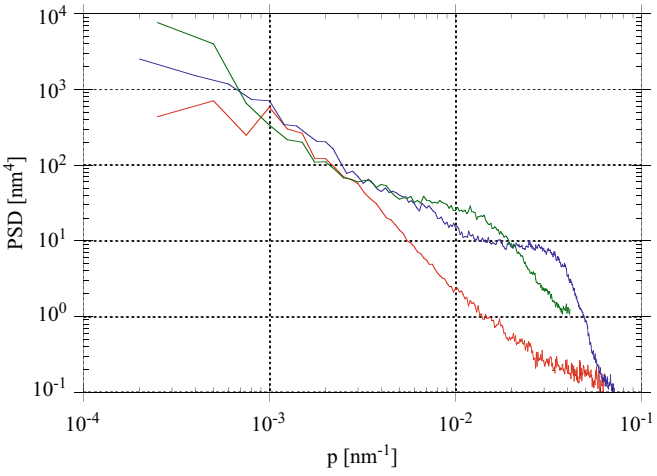

Fig. 3. Comparison of the PSD functions taken after ion irradiation at 10° (blue), 45° (red) and 90° (green) grazing angles. The different spatial frequency ranges result from different sampling distances and scanning windows used while recording the AFM images. (For interpretation of the references to colour in this figure legend, the reader is referred to the web version of this article.)

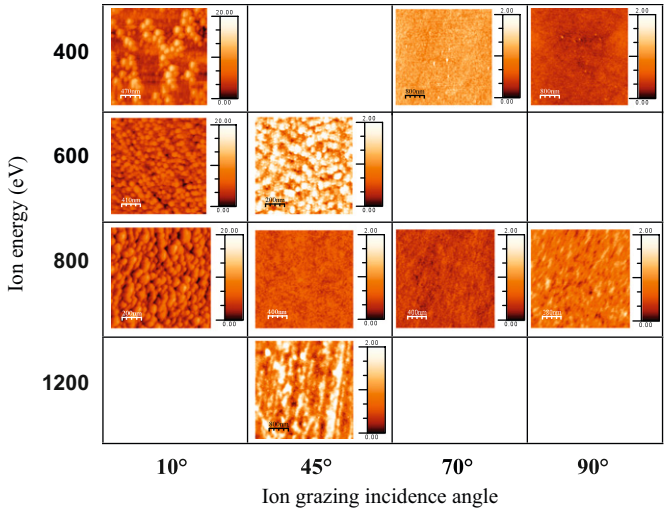

Fig. 4. AFM images recorded at the center of the irradiated zone for a series of silicon wafer substrates irradiated at various grazing angles (10°, 45°, 70°, 90°) and ion energy (400, 600, 800, 1200 eV).

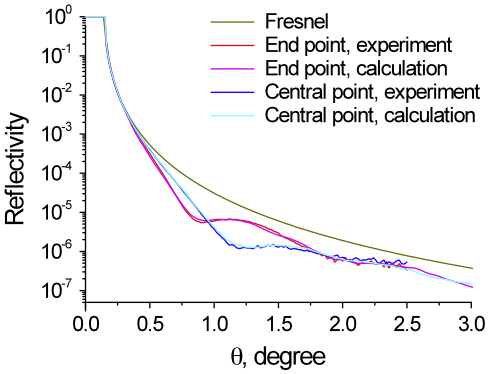

Fig. 5. Reflectivity profiles as a function of the angle measured at the center and the edge of the mirror at an X-ray energy of 12 keV. The greenish curve corresponds to the Fresnel case.

Two elliptical cylinder mirrors with a strong aspherization were figured with ions, see Ref. [9]. A series of measurements of the X-ray reflectivity profile were performed with the X-ray beam direction coinciding with the cylinder axis, i.e., orthogonal to the plane of incidence of the eventual nanofocusing application of these mirrors. The reflectivity profiles were recorded as a function of the grazing angle of incidence between 0° and 3° at 5 mm intervals along the ellipse. Fig. 5 shows the reflectivity profiles for two particular positions, at the center of the mirror and at one of the edges. Their analysis using the approach described in Ref. [13] allowed us to reconstruct the density depth profile and its evolution. The density of the silicon was found to be practically constant regardless of the depth (Fig. 6a) except at the top of the surface (z=0). There, we observed the presence of an adhesion layer approximately 1.5 nm thick in the center of the mirror and varying by 0.6 nm when moving to the outer region, unexposed to ions. Fig. 6b shows AFM images recorded over an area of 5 μm^2 at the center of the area exposed to the ion beam and at the edge of the mirror. Although the eroded depth varied from 10 μm at the center to a negligible value at the edge of the eroded zone the rms roughness was nearly the same, of the order of 0.15 nm. At an angle of 6 mrad (0.34°), i.e., at the design value of X-ray mirror operation, the reflectivity (Fig. 5) practically coincides with the value obtained using the Fresnel formula. Thus, the reflectivity decrease caused by the roughness would be acceptable for X-ray reflective optics applications. The images shown in Fig. 7 were taken with the interferential microscope using fields of $1.3\times0.8\,mm^2$ (magnification 5×, resolution 2.5 μm) and $130\times83\,\mu m^2$ (magnification 50×, resolution 0.5 μm). The rms values averaged over four points randomly distributed over the treated surface within the image are of 0.48 nm (5×) and 0.18 nm (50×). The larger value observed with the largest field of view is mostly due to the presence of isolated defects (flakes). As for the AFM measurements, the roughness was found to be nearly independent of the erosion depth and with an isotropic distribution that can be well described by a Gaussian profile. The roughness values are consistent with those obtained on the virgin samples, i.e., prior to ion treatment, and also closely agree with results reported by other authors treating surfaces with low-energy ions [14].

4. Conclusion

The results presented demonstrated that a roughness level below 0.2 nm can be preserved in a wide range of lateral lengths, i.e., over spatial periods up to 130 μm, and for etching times exceeding 4 h. These results anticipate the possibility of generating substrates with

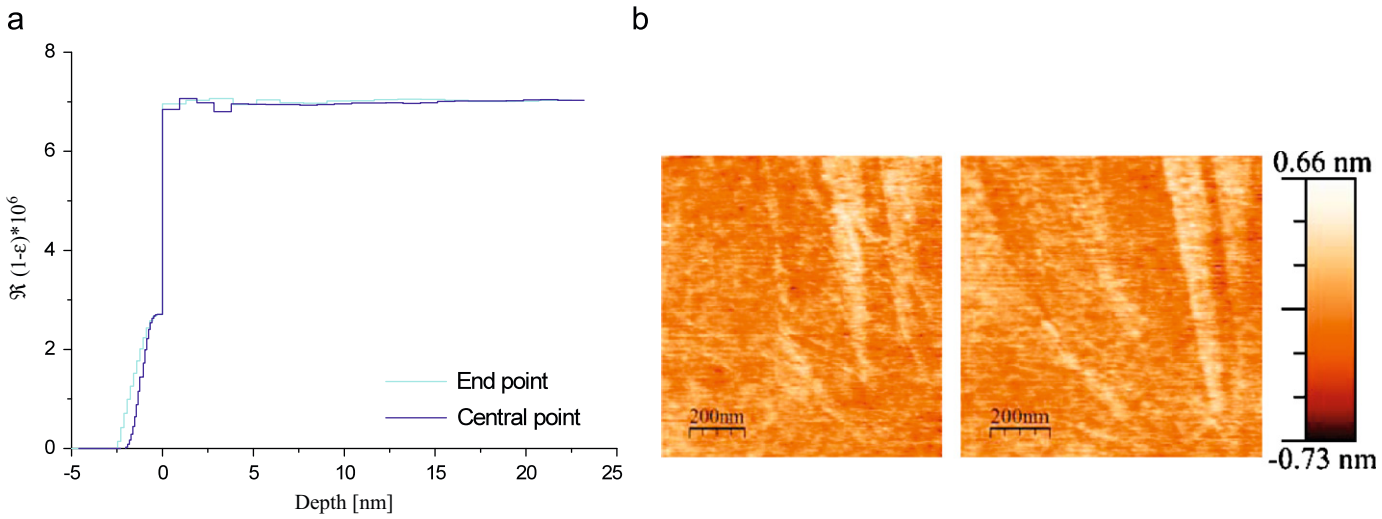

Fig. 6. (a) Depth-distribution of silicon density extracted using of the approach described in Ref. [11] from reflectivity profiles measured in the center and at the end of the irradiated region. The bump of the left side of the curves corresponds to the presence of an adhesion layer. (b) AFM topographs measured at the mirror center (left) and at the edge (right) of the mirror. The rms roughness values are 0.15 and 0.14 nm, respectively.

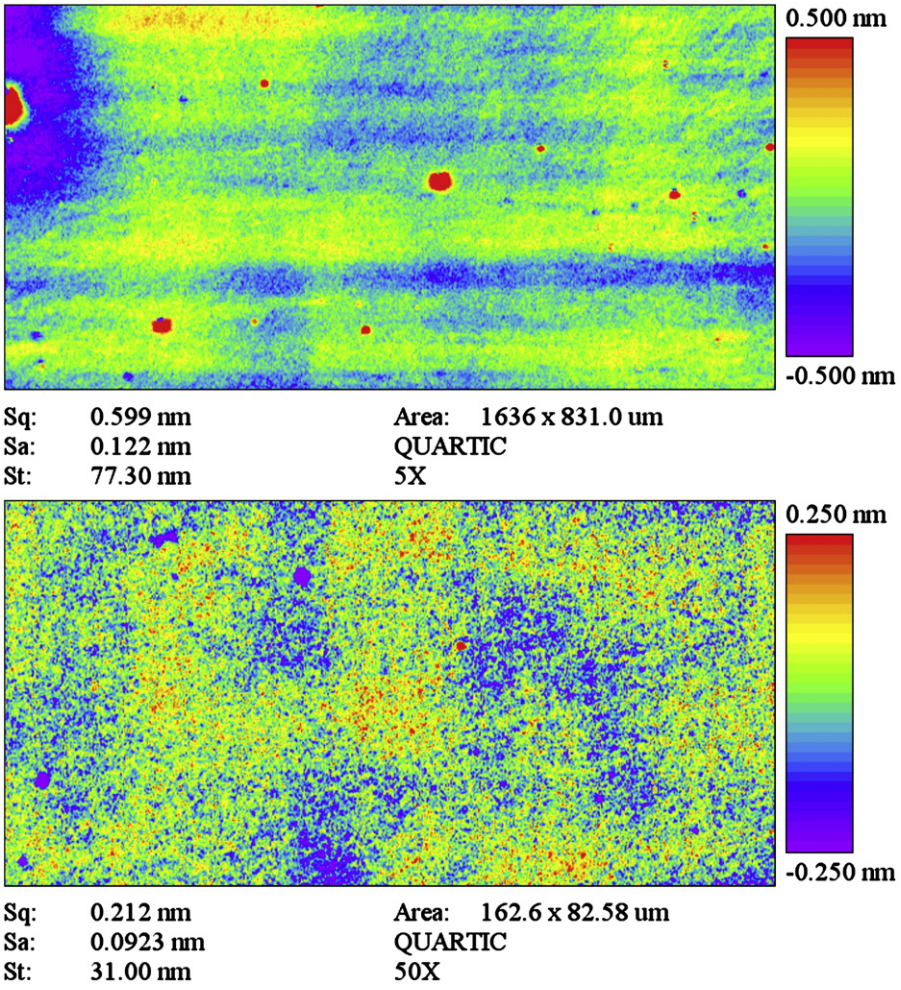

Fig. 7. Images taken with an interferential microscope Promap 512. Left: probed area: $1.3 \times 0.8\ mm^2$, magnification $5\times$, resolution 2.5 μm, rms roughness: 0.60 nm. Right: probed area: $130 \times 83\ \mu m^2$, magnification $50\times$, resolution 0.5 μm, rms roughness: 0.21 nm. The roughness values averaged over 4 different areas are 0.48 nm ($5\times$) and 0.18 nm ($50\times$).

a surface finish compatible with multilayer deposition and suitable for nanofocusing. In the future, online at-wavelength diagnostics will be preferred [8] eliminating at the same time the recurrent problem of reproducibility of sample positioning within the metrology and surfacing tools. As surface finish (roughness) directly affects the amount of light that is scattered, an X-ray scattering

diagnostic tool will obviously be the most relevant parameter to monitor. This diagnostic is also compatible with the ion beam process as it is a non-contact method.

Acknowledgements

We gratefully acknowledge the assistance of S. Guillet, J-Y. Massonnat, G. Rostaing and P. van Vaerenbergh during the design and manufacturing phases of the experimental station, the help from the ESRF ISDD BCU group and J-Y. Massonnat during beamline measurements, and the assistance of Simon Le Denmat and Florence Marchi from the ESRF Surface Science Lab during AFM measurements. I.V. Kozhevnikov acknowledges the support of the ISTC (Project no. 3124).

References

[1] Purple Book: Science and Technology Programme 2008–2017, in: ESRF editor (2007), 〈http://www.esrf.eu/files/Upgrade/ESRF-SciTechProg2008-2017-lr.pdf〉.
[2] Y. Mori, K. Yamauchi, K. Yamamura, H. Mimura, Y. Sano, A. Saito, A. Souvorov, K. Tamasaku, M. Yabashi, T. Ishikawa, Jpn. Soc. Precis. Eng. 68 (10) (2002) 1347;
Y. Takahashi, Y. Nishino, R. Tsutsumi, H. Kubo, H. Furukawa, H. Mimura, S. Matsuyama, N. Zettsu, E. Matsubara, T. Ishikawa, K. Yamauchi, Phys. Rev. B 80 (2009) 054103.
[3] R. Soufli, S. Baker, D. Windt, E. Gullikson, J. Robinson, W. Podgorski, L. Golub, Appl. Opt. 46 (16) (2007) 3156.
[4] L. Peverini, E. Ziegler, T. Bigault, I. Kozhevnikov, Phys. Rev. B 76 (4) (2007) 045411.
[5] J. Susini, Opt. Eng. 34 (2) (1995) 361.
[6] E. Spiller, Opt. Eng. 29 (6) (1990) 609;
A. Schindler, T. Haensel, A. Nickel, H.J. Thomas, H. Lammert, F. Siewert, SPIE Proc. 5180 (2004) 64.
[7] F. Frost, B. Ziberi, A. Schindler, B. Rauschenbach, Appl. Phys. A 91 (2008) 551.
[8] E. Ziegler, L. Peverini, I. Kozhevnikov, T. Weitkamp, C. David, in: J.Y. Choi, S. Rah (Eds.), AIP Conference Proceedings, vol. 879 (2006) 778.
[9] L. Peverini, et al., Ion beam profiling of aspherical X-ray mirrors, in this issue.
[10] J.M. Elson, J.M. Bennett, Appl. Opt. 34 (1) (1995) 201.
[11] Silicon substrates manufactured by General Optics, Gooch & Housego, Moorpark, CA, USA.
[12] Windows software program developed by Nanotec Electronica S.L., Spain (〈http://www.nanotec.es〉).
[13] I.V. Kozhevnikov, Nucl. Instr. and Meth. A 508 (3) (2003) 519.
[14] F. Frost, R. Fechner, B. Ziberi, D. Flamm, A. Schindler, Thin Solid Films 459 (2004) 100.